JACS
JOURNAL OF THE AMERICAN CHEMICAL SOCIETY
Article
pubs.acs.org/JACS

Bimolecular Photoinduced Electron Transfer in Imidazolium-Based Room-Temperature Ionic Liquids Is Not Faster than in Conventional Solvents

Marius Koch,[†] Arnulf Rosspeintner,[†] Gonzalo Angulo,[‡] and Eric Vauthey*[,†]

[†]Department of Physical Chemistry, University of Geneva, 30 Quai Ernest-Ansermet, 1211, Genève 4, Switzerland
[‡]Institute of Physical Chemistry, Polish Academy of Sciences, Kasprzaka 44/52, 01-224 Warsaw, Poland

Supporting Information

ABSTRACT: The fluorescence quenching of 3-cyanoperylene upon electron transfer from *N*,*N*-dimethylaniline in three room-temperature ionic liquids (RTILs) and in binary solvent mixtures of identical viscosity has been investigated using steady-state and time-resolved fluorescence spectroscopy. This study was stimulated by previous reports of bimolecular electron transfer reactions faster by one or several orders of magnitude in RTILs than in conventional polar solvents. These conclusions were usually based on a comparison with data obtained in low-viscous organic solvents and extrapolated to higher viscosities and not by performing experiments at similar viscosities as those of the RTILs, which we show to be essential. Our results reveal that (i) the diffusive motion of solutes in both types of solvents is comparable, (ii) the intrinsic electron transfer step is controlled by the solvent dynamics in both cases, being slower in the RTILs than in the conventional organic solvent of similar viscosity, and (iii) the previously reported reaction rates much larger than the diffusion limit at low quencher concentration in RTILs originate from a neglect of the static and transient stages of the quenching, which are dominant in solvents as viscous as RTILs.

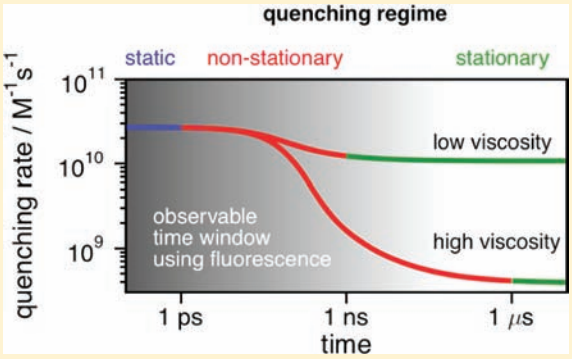

INTRODUCTION

The interest in room-temperature ionic liquids (RTILs) as nonvolatile, thermally stable, and conductive solvents has undergone an impressive increase over the past few years.[1−4] These properties, together with the broad electrochemical window and a very good solubility for both organic and inorganic solutes, have turned RTILs into promising alternatives to "conventional" solvents in fields as diverse as organic synthesis[2,4] or solar energy conversion.[3,5−7]

Besides these potential applications, many efforts have been made to obtain a deeper understanding of the possible intrinsic differences of elementary processes in ionic and conventional liquids.[8,9] In particular, electron transfer (ET), constituting the simplest and, at the same time, one of the most ubiquitous chemical reactions, has been the subject of studies yielding surprising and unexpected results. Intramolecular ET reactions have not been found to show any markedly different behavior in RTILs than in conventional solvents,[10−12] whereas just the opposite was reported for their bimolecular analogues. Most of the previous works on ET in RTILs reported extremely accelerated reaction rates compared to conventional solvents.[13−18] Indeed, the ET reactions in conventional solvents were observed to be diffusion controlled, while quenching rate constants up to 2 orders of magnitude larger than diffusion were found in RTILs. These extraordinary findings have been given different explanations, ranging from accelerated diffusion[13,14] and ET occurring in the alkyl chain regions of the RTIL,[15] to a tentative statement on too simplified a data analysis.[9,12]

The interpretations of the results obtained in RTILs are very often based on the assumption that the measured rate constant is simply equal to the diffusion rate constant and should therefore be inversely proportional to the solvent viscosity, which is indeed very high for RTILs. However, this view of a fluorescence quenching process is much too simplistic and only valid at very low quencher concentrations and in nonviscous solvents. In fact, as illustrated in Figure 1, in a diffusion-controlled bimolecular quenching process, the quenching rate, k, is not constant but decreases continuously over time from a value k_0, which is the intrinsic, diffusion-free, ET rate constant, until it reaches a constant value corresponding to the diffusion-controlled rate constant, k_{diff}.[19−26] In a first approximation, that is, assuming spherical reactants of identical radius and contact quenching distance, r_0, k_{diff} is given by

$$k_{diff} = 4\pi r_0 D N_A = \frac{8\cdot 10^6 RT}{3\eta} \quad (1)$$

Received: September 1, 2011
Published: January 27, 2012

   dx.doi.org/10.1021/ja208265x | *J. Am. Chem. Soc.* 2012, 134, 3729−3736

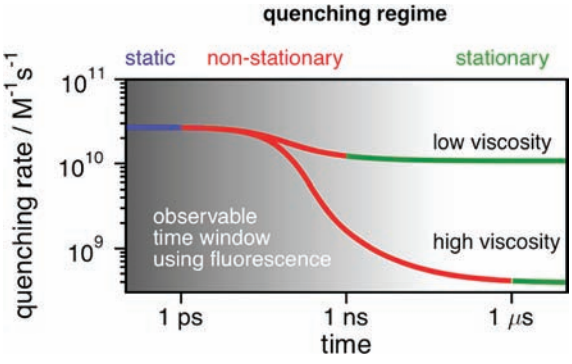

Figure 1. Illustration of the three quenching regimes in a low and high viscosity solvent. The shading represents the time-dependent probability of finding a fluorophore in the S_1 state after optical excitation at time zero in the absence of quencher in the solution.

where D is the mutual diffusion coefficient and η is the viscosity in cP.

The time dependence of the rate is due to the existence of three distinct quenching regimes: (1) Directly after optical excitation of the fluorophores, the quenching is *static* and takes place between the reactant pairs that are already at optimal distance. In this case, no diffusion is necessary and thus the quenching rate is the intrinsic ET rate, k_0, which remains constant during this process (blue lines in Figure 1). (2) Once these pairs have reacted, quenching occurs between reactant pairs that are further and further apart and which have time to undergo some diffusion. In other words, a hole created by the reaction in the pair distribution distance between fluorophore and quencher molecules gradually increases (see Figure S2 in the Supporting Information). This continues as long as there is no equilibrium between the rate at which the intrinsic reaction occurs and the rate at which the pairs approach each other sufficiently to react. This is the so-called *non-stationary* or *transient regime*, during which the reaction rate constantly decreases with time (red lines in Figure 1). (3) Eventually, the remaining reactants are so far apart that quenching is only possible after substantial diffusion and an equilibrium between this diffusional formation of the reactant pairs and their decay upon reaction is attained, giving rise to a constant reaction rate. This constitutes the so-called *stationary regime* of the reaction with the stationary rate constant, k_{diff} (green lines in Figure 1). The duration of the static regime is directly related to the intrinsic rate constant, k_0, whereas that of the transient regime depends on the diffusion coefficient and thus on the viscosity of the solution. As a consequence, in a highly viscous solvent, such as RTILs, the stationary regime may only be reached after several hundreds of nanoseconds. Therefore, if the excited-state lifetime of the fluorophore amounts to a few nanoseconds, as it is usually the case, the stationary regime is never established. One can also see that not only the duration but also the amplitude of the nonstationary regime, that is, the difference between k_0 and k_{diff}, increases with solvent viscosity. Therefore, whereas too simplistic an analysis of the quenching data may have little consequence in a low viscosity solvent, it may lead to erroneous conclusions in a high viscosity solvent like a RTIL.

In order to find out whether the aforementioned unusually fast quenching in RTILs is an intrinsic property of these solvents or only the result of an improper data analysis, we have investigated the fluorescence quenching of 3-cyanoperylene (CNPe) by *N*,*N*-dimethylaniline (DMA) in three RTILs of different viscosities (Chart 1) using steady-state and subnanosecond time-resolved fluorescence spectroscopy, that is, time-correlated single photon counting (TCSPC), to construct Stern–Volmer plots. The results were compared to those obtained in binary solvent mixtures of dimethylsulfoxide (DMSO) and glycerol (GLY) with viscosities identical to those of the RTILs. DMSO/GLY mixtures have already been used to study the influence of viscosity on photoinduced ET and other bimolecular reactions. These mixtures have the advantage that, at least macroscopically, many physical quantities, such as dielectric constant, refractive index, or density, remain unchanged over a wide range of molar fractions and thus viscosity.[27−32]

Chart 1. Structures and Properties (at 20°C) of the Fluorophore, Quencher and Solvents[a]

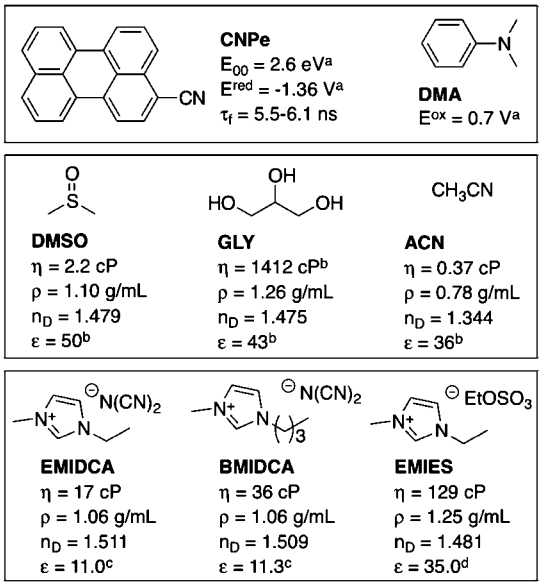

[a](a) From ref 33, (b) from ref 34, (c) from ref 35, and (d) from ref 36.

Additionally, femtosecond time-resolved measurements by fluorescence up-conversion were performed in one RTIL and one DMSO/GLY mixture to investigate the static and transient quenching regimes. Control measurements were performed in a low viscous organic polar solvent, acetonitrile.

We will show that (i) the diffusive motion of the reactants is very similar in RTILs and conventional solvents of comparable viscosity, (ii) the intrinsic ET reaction is solvent controlled, that is, slower than in conventional low viscous solvents, (iii) the previously observed accelerated reaction rates are indeed artifacts of an oversimplified data treatment as suggested by Li et al.,[12] and (iv) the ET quenching of CNPe in viscous solvents takes place mostly in the static and transient regimes and should thus be analyzed with a model that can properly account for these regimes, like, for example, differential encounter theory (DET).[26]

EXPERIMENTAL SECTION

a. Chemicals. 3-Cyanoperylene (CNPe) was synthesized according to the literature[37] and purified by column chromatography. *N*,*N*-dimethylaniline (DMA) was obtained from Fluka (puriss p.a., 99.5%), distilled under reduced pressure, and stored under argon.

Glycerol (GLY, Alfa Aesar, ultrapure, HPLC grade) was stored water-free under argon and used as received. Dimethylsulfoxide

dx.doi.org/10.1021/ja208265x | J. Am. Chem. Soc. 2012, 134, 3729–3736

(DMSO, Fisher Scientific, U.K., 99.7%) was purified by performing two freezing cycles, in which the remaining liquid portion of about 10% was separated from the frozen DMSO. Acetonitrile (ACN, Roth, ≥99.9%) was stored over a molecular sieve (Aldrich, 3 Å) and under argon.

The room temperature ionic liquids (RTILs), 1-ethyl-3-methylimidazolium dicyanamide (EMIDCA, >98%), 1-butyl-3-methylimidazolium dicyanamide (BMIDCA, >98%), and 1-ethyl-3-methylimidazolium ethylsulfate (EMIES, >99%), were purchased from IoLiTec (Germany) and heated at 80−100 °C under reduced pressure (2 mbar) for 3 h before use. The water content of the RTILs was determined by Karl Fischer titration (EMIDCA < 200 ppm, BMIDCA < 300 ppm, EMIES < 800 ppm).

b. Characterization of the Solutions. The viscosities of the DMSO/GLY mixtures and the RTILs were measured using an Ubbelohde viscosimeter (SI Analytics GmbH, Germany, type IIc), taking the mean of three individual measurements. Both solvent and viscosimeter were allowed to reach the measurement temperature of 20 ± 0.1 °C over a period of 30 min.

CNPe solutions were prepared at least one day before carrying out the experiments to ensure complete dissolution of the fluorophore. All samples were handled under argon throughout the entire preparation and experimental procedure.

For the entire set of experiments, emission from the RTILs was negligible at the used settings. The DMSO/GLY mixtures and ACN did not show any emission. Neither sample degradation nor changes of spectral shape and position were observed upon increasing the quencher concentration in all types of solvents. Thus both exciplex and ground-state complex formation can be excluded.

c. Steady-State Measurements. Absorption spectra were recorded on a Cary 50 spectrophotometer, whereas fluorescence spectra were measured on a Cary Eclipse fluorimeter (step size: 2 nm, excitation slit: 5 nm, emission slit: 2.5 nm). Both experiments were performed using septum sealed 10 mm quartz cuvettes. A more detailed description of the polarization dependent data recording and data treatment can be found in the Supporting Information. In essence, the polarization dependence of the detection system in any fluorimeter can make a proper control of the excitation and emission polarization necessary to obtain correct quenching results.

d. Time-Resolved Fluorescence. Subnanosecond time-resolved fluorescence decays were measured using the time-correlated single photon counting (TCSPC) technique with a setup similar to that described in ref 38. Briefly, excitation at a repetition rate of 10 MHz was performed using a laser diode (Picoquant model LHD-D-C-470) at 470 nm with a pulse duration of 60 ps. The full width at half-maximum (FHWM) of the instrument response function was about 200 ps. Linearly polarized excitation was ensured by passing the excitation beam through a Glan-Taylor polarizer. The emission was collected at magic angle after passing through an interference filter of 9 nm bandwidth at a central wavelength of 520 nm. The absorbance of the sample solution was kept below 0.5 at the excitation wavelength in a 10 mm septum sealed cuvette.

Femtosecond time-resolved fluorescence decays were monitored using a fluorescence up-conversion setup as described in ref 39. Excitation was performed at 440 nm (Mai-Tai, Spectra Physics) with a repetition rate of 80 MHz. For the emission, 520 and 525 nm wavelengths were chosen for RTIL and DMSO/GLY, respectively, the effective bandpass being 25 nm. At these wavelengths, the contribution of vibrational cooling and/or dynamic solvent shift was minimal and allowed an almost unperturbed observation of the excited CNPe population decay. Nonetheless, the time-decays in the presence of quencher were corrected for the slightly nonexponential intrinsic fluorophore decay before comparison with the model. The FWHM of the instrument response function was 250 fs as determined from the rising edge of the pure CNPe signal. The CNPe concentration was adjusted to obtain an absorbance of less than 0.3 at the excitation wavelength on an optical path length of 0.45 mm in a rotating cell.

RESULTS AND DISCUSSION

a. ET Quenching and Simple Stern−Volmer Analysis. The fluorescence decay of CNPe in all solvents investigated is strongly accelerated upon addition of DMA, examples being shown in Figure 2. In this figure, the experimentally measured

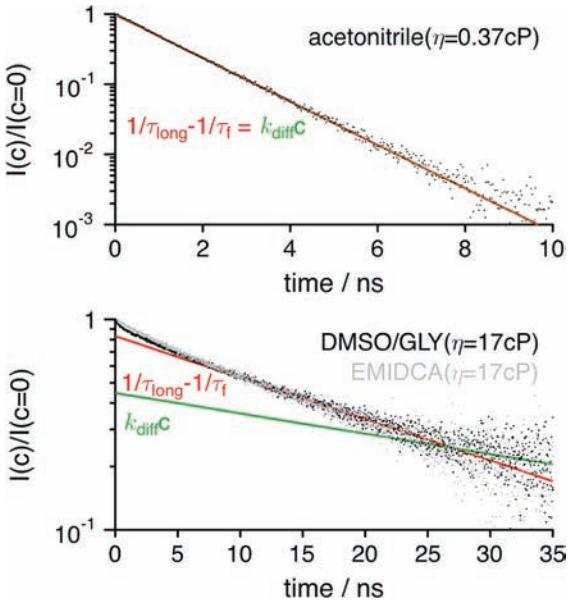

Figure 2. Pure fluorescence quenching kinetics (corrected for the intrinsic natural fluorophore decay) measured by TCSPC upon excitation of CNPe at 470 nm in the presence of 0.047 M DMA in acetonitrile (top panel) EMIDCA and a mixture of DMSO/GLY of 17 cP (bottom panel). The red and green lines are exponential decays using the slowest component of a multiexponential fit, τ_{long}, to the experimental data (red) and the stationary rate constant, obtained from DET (see text below and Supporting Information), $(k_{diff}c)^{-1}$, respectively.

time profiles, $I(t,c)$, have been divided by that recorded without DMA, $I(t,c=0)$, to better appreciate the effect of the quencher.[40] The mechanism underlying the quenching of CNPe by DMA is an electron transfer from the amine to CNPe in the S_1 state, as confirmed by femtosecond transient absorption spectra recorded after excitation of CNPe at 400 nm. They clearly show the concomitant decay of CNPe in the S_1 state and the formation of the $CNPe^-$ radical anion (see Figure S5 in the Supporting Information). The radical cation of DMA absorbs comparatively too weakly to be observed. This result also agrees with the calculated driving force for ET, which is larger than 0.3 eV in all the solvents used here.

The fluorescence quenching kinetics in ACN is exponential (Figure 2), while those recorded in the RTILs and in the DMSO/GLY mixtures require the sum of several exponential functions to be satisfactorily reproduced. If we assume that the slowest decay component with a lifetime τ_{long} corresponds to the stationary regime, the following Stern−Volmer equation can be formulated:

$$\frac{\tau_f}{\tau_{long}(c)} = 1 + K_{SV}^{\tau}c = 1 + k_q^{\tau}\tau_f c \qquad (2)$$

where K_{SV}^{τ} is the Stern−Volmer constant and k_q^{τ} is the experimental quenching rate constant, which, in the stationary regime, should be equal to the diffusion rate constant, k_{diff}. The superscript "τ" denotes that these values have been determined

dx.doi.org/10.1021/ja208265x | J. Am. Chem. Soc. 2012, 134, 3729−3736

from the decay times. The k_q^τ values were obtained from the slope of the Stern–Volmer plots of τ_f/τ_{long} versus DMA concentration as shown in Figure 3. They are listed in Table 1 together with the k_{diff} values estimated using eq 1.

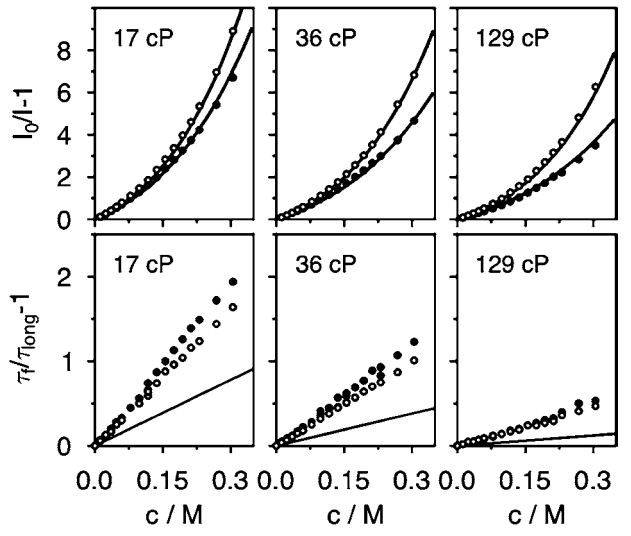

Figure 3. Steady-state (upper panels) and time-resolved (lower panels) Stern–Volmer plots for the ET quenching of CNPe by DMA in three RTILs (black dots) and DMSO/GLY mixtures (open circles) of identical dynamic viscosities. The lines are best fits using DET with the parameters given in Table 2. The Stern–Volmer plots with k_{diff}, obtained from DET (see text below and Supporting Information), are shown in the lower panels and are indistinguishable in both types of liquids for a given viscosity.

Table 1. Experimentally Obtained Quenching Rate Constants, k_q^τ and k_q^s, and the Diffusional Rate Constant, k_{diff}, As Calculated from eq 1

	k_q^τ, 10^9 M^{-1} s^{-1}	k_q^s, 10^9 M^{-1} s^{-1}	k_{diff}, 10^9 M^{-1} s^{-1}
ACN	17	18	18
EMIDCA	1.1	1.6	0.38
DMSO/GLY (17 cP)	0.99	1.9	0.38
BMIDCA	0.70	1.3	0.18
DMSO/GLY (36 cP)	0.60	1.4	0.18
EMIES	0.28	1.0	0.050
DMSO/GLY (129 cP)	0.27	1.3	0.050

This table reveals an excellent agreement between k_q^τ and k_{diff} in ACN but strong discrepancies in all RTILs and DMSO/GLY mixtures, where k_q^τ is substantially larger than the calculated diffusion rate constant. In the RTILs, the k_q^τ/k_{diff} ratio increases from 3 to 5.6 by going from the least to the most viscous solvent. Such a quenching rate constant faster than diffusion in RTILs agrees with previous reports, although the difference is somewhat smaller. However, this effect does not seem to be related to the ionic nature of the solvents, because a similar discrepancy, that is, a $k_q^\tau/k_{diff} > 1$, is observed in the DMSO/GLY mixtures as well. Here the ratio increases from 2.6 to 5.6 by going from the 17 to the 129 cP mixture. As a consequence, this effect cannot be due to any unique property of RTILs but rather originates from the high viscosity.

The quenching rate constant can also be extracted by considering the decrease of the steady-state fluorescence intensity, I_{ss}, upon addition of quencher:

$$\frac{I_{ss}(c=0)}{I_{ss}(c)} = 1 + K_{SV}^s c = 1 + k_q^s \tau_f c \quad (3)$$

where the superscript "s" specifies that these values originate from a so-called steady-state Stern–Volmer plot. These plots, performed for the CNPe fluorescence quenched by DMA in ACN, RTILs, and DMSO/GLY mixtures, are shown in Figures 3 and 4. Although eq 3 predicts a linear dependence of the

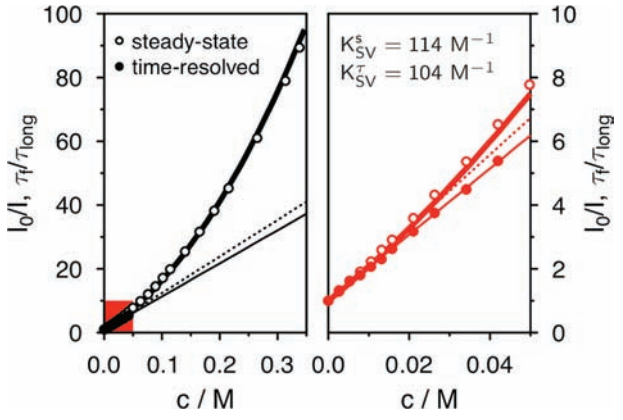

Figure 4. Steady-state and time-resolved Stern–Volmer plots for the CNPe/DMA pair in acetonitrile. The right graph is an expanded view of the low concentration data. The bold solid line has been calculated using DET with the parameters listed in Table 2. The thin solid and dashed lines are linear fits to the time-resolved and low concentration steady-state data, respectively. K_{SV} indicates the so obtained Stern–Volmer constants ($K_{SV}^\tau = \tau_f k_q^\tau$, $K_{SV}^s = \tau_f k_q^s$).

fluorescence intensity ratio on the quencher concentration, a strongly nonlinear behavior is observed in all solvents. At constant viscosity, the curvature of the Stern–Volmer plot is even larger in the DMSO/GLY mixture than in the RTIL. This deviation from linearity is a direct manifestation of the static and transient quenching regimes that will be discussed in more detail below. In fact, a similar result would be obtained from the "time-resolved" Stern–Volmer analysis, eq 2, using the average decay time instead of τ_{long}. As the contribution of both static and transient regime increases with quencher concentration, the Stern–Volmer constant, K_{SV}^s, and k_q^s depend on the quencher concentration. This effect is well-known and, to avoid it, eq 3 is usually used at low quencher concentrations only, where the dependence is mostly linear.

The quenching rate constants, k_q^s, obtained using eq 3 at low quencher concentrations are also listed in Table 1. In ACN, k_q^s is essentially equal to k_q^τ and to k_{diff}, indicating that the contribution of static and transient quenching regimes is negligible when using eq 3 in the low concentration limit. On the other hand, in the RTILs, the discrepancy between k_q^s and k_{diff} is even larger than that already found with k_q^τ. Indeed, the k_q^s/k_{diff} ratio increases from 4.2 to 20 when going from the least to the most viscous RTIL. Here again, this effect is not intrinsic to the RTILs, as it is also present in the DMSO/GLY mixtures, where the k_q^s/k_{diff} ratio changes from 5 to 26.

Both time-resolved and steady-state Stern–Volmer plots reveal that the quenching is more efficient in the DMSO/GLY mixtures than in the RTILs of the same viscosity. This points

dx.doi.org/10.1021/ja208265x | J. Am. Chem. Soc. 2012, 134, 3729–3736

toward a slower ET in the latter solvents. The observed difference increases with the quencher concentration and the solvent viscosity. This finding is substantiated by the early quenching dynamics measured by fluorescence up-conversion in EMIDCA and DMSO/GLY of 17 cP after excitation with femtosecond laser pulses (Figure 5). Clearly, the early stage of

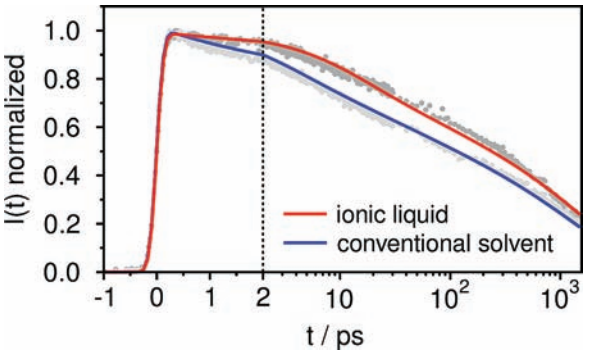

Figure 5. Fluorescence up-conversion profiles measured with CNPe in the presence of 0.23 M DMA in EMIDCA (dark gray dots and red line) and a 17 cP DMSO/GLY mixture (light gray dots and blue line). The lines show the best fits of DET with the parameters listed in Table 2.

the reaction is faster in the solvent mixture than in the RTIL. However, after about 10 ps, both fluorescence profiles exhibit an almost parallel decay. This can also be seen in the nanosecond quenching profiles (Figure 2) and points toward very similar diffusion coefficients in both types of liquids. This apparent similarity of translational diffusion coefficients is further supported by identical femtosecond time-resolved fluorescence anisotropy decays of CNPe (Figure S4 in the Supporting Information), pointing to very similar reorientational dynamics in both types of solvents.

In summary, we find from the above model-free data analysis that the ET quenching in RTILs is not faster than in polar organic solvent mixtures of similar viscosities. Moreover, apart from ACN, the quenching rate constants deduced for a simple Stern–Volmer analysis of the fluorescence quenching are much larger than the diffusion rate constants. A similar result has already been reported in RTILs and has been ascribed to some specific property of these solvents. However, our measurements reveal that the same effect takes place in conventional dipolar solvents of similar viscosity. Thus, the ionic nature of the solvent cannot be invoked to account for this phenomenon.

b. Data Analysis Using Differential Encounter Theory. The above results indicate that a Stern–Volmer analysis using eqs 2 and/or 3 cannot properly account for the quenching of CNPe fluorescence in viscous solvents. Indeed, these equations are only valid in the stationary regime where k_q is constant. Because of this, either the initial part of the quenching dynamics or the quenching data measured at high concentrations, where both the static and transient stages of the quenching are dominating, have to be omitted. As shown in Figure 1, the more viscous the solution, the longer the duration and amplitude of the transient regime where the quenching rate changes from the intrinsic ET rate, k_0, to the diffusion rate constant, k_{diff}.

A crude estimate of the lower limit for the duration of the transient regime is given by the encounter time, $\tau_e = r_q^2/D$, where r_q is the quenching radius. This time is approximately the duration of an encounter of the two reactants where they experience the same solvent fluctuations. The fluorescence decay in ACN as shown in Figure 2 indicates that the stationary regime is being approached within the time-resolution of the experiment, which is of the order of 200 ps. This is in good agreement with an encounter time of about 150 ps, calculated assuming contact quenching ($r_q = r_0$). On the other hand, the encounter times calculated for solvents of 17, 36, and 129 cP amount to 1, 2, and 7 ns, respectively. Comparing these values with the fluorescence lifetime of CNPe indicates that the transient regime dominates the quenching of CNPe by DMA in the RTILs and the DMSO/GLY mixtures.

A full account of the quenching dynamics requires the application of a model allowing the analysis of all three quenching regimes. We will use here the so-called differential encounter theory,[26] that, contrary to the more popular Collins–Kimball model,[41] allows for any distance dependence of the ET process. In DET, the time profile of the fluorescence intensity is given by:

$$I(t) = I(0)\exp\left[-\frac{t}{\tau_f} - c\int_0^t k(t')\,dt'\right] \quad (4)$$

where $k(t)$ is no longer a constant and is thus called quenching rate coefficient. The latter can be expressed as

$$k(t) = 4\pi\int_{r=r_0}^{\infty} w(r)n(r,t)r^2\,dr \quad (5)$$

where $w(r)$ is the reaction probability that depends on the inter-reactant distance, r, and $n(r,t)$ is the reactant pair distribution function (see the Supporting Information for further details). The time dependence of this distribution function is at the origin of the transient effect. During the static and transient stages of the quenching, the pair distribution at short r decreases continuously until the equilibrium between the disappearance of the pairs by quenching and their formation by diffusion is established. From then on, the pair distribution function is independent of time and the stationary quenching regime is reached. When determining $n(r,t)$, one should consider that the solvent–solvent pair distribution function of molecular liquids is not flat at short distances due to the excluded volume effect.[42] As a consequence, it is more likely to find reactant pairs in close contact than at slightly larger distances. Eventually, at large interparticle distances, this effect disappears and gives rise to a homogeneous distribution function. This effect, which basically translates into an increased effective concentration of close pairs compared to the bulk concentration,[32] enhances the reaction rate in the static regime and has to be taken into account. Moreover, the diffusion between reactants is not homogeneous either, due to the hydrodynamic hindering of the mutual diffusion. In simple words, whenever two reactant molecules approach each other, they feel a drift force directed in the opposite direction, which decreases the mutual diffusion coefficient at short distances. The detail of the determination of the reactant pair distribution taking into account these latter two effects is discussed in the Supporting Information.

The reaction probability, $w(r)$, was modeled using Marcus ET theory (eq. S9 in the Supporting Information).[43] Because of the high viscosity of the solvents used here, their finite dielectric response time, τ_L, was included in the preexponential factor.[44−47] For ACN, this value has been taken from the literature,[48] whereas for the RTILs, this quantity has been adjusted. Finally, for DMSO/GLY, a constant value that has

dx.doi.org/10.1021/ja208265x | J. Am. Chem. Soc. 2012, 134, 3729–3736

Table 2. Input and Best-Fit Parameters Obtained from the Analysis of the Time-Resolved Fluorescence and Steady-State Stern–Volmer Plot Using eq 4[a]

	ACN	EMIDCA	BMIDCA	EMIES	DMSO/GLY 17 cP	DMSO/GLY 36 cP	DMSO/GLY 129 cP
r_0, Å	6.6	7.0 ± 0.1	7.0 ± 0.1	7.0 ± 0.1	7.0 ± 0.1	7.0 ± 0.1	7.0 ± 0.1
V_0, meV	31	28 ± 1	28 ± 1	28 ± 1	29 ± 1	29 ± 1	29 ± 1
β, Å^{-1}	1.08	1.14 ± 0.03	1.14 ± 0.03	1.14 ± 0.03	1.11 ± 0.03	1.11 ± 0.03	1.11 ± 0.03
ΔG, eV	−0.53	−0.31	−0.33	−0.53	−0.56	−0.56	−0.56
τ_L, ps	0.3	4	8	28	0.8	0.8	0.8
λ_s, eV	0.86	0.72	0.73	0.88	0.88	0.88	0.88
D, Å^2 ns^{-1}	350	7.3	3.3	1.0	7.3	3.3	1.0
k_0, 10^9 M^{-1} s^{-1}	580	80	40	15	380 ± 40	380 ± 40	380 ± 40

[a] r_0: contact radius; V_0: coupling matrix element at r_0; β: attenuation constant; ΔG: driving force at r_0 calculated using Supporting Information eq (S14); τ_L: longitudinal dielectric relaxation time; λ_s: reorganization energy at r_0; D: mutual diffusion coefficient at infinite reactant separation; k_0: intrinsic ET rate constant.

successfully been used in the past regardless of the viscosity of the solvent mixture was assumed.[32] The distance dependence of $w(r)$ was expressed in the electronic coupling matrix element, V,

$$V(r) = V_0 \exp[-\beta(r - r_0)/2] \quad (6)$$

where β is an attenuation coefficient, as well as in the solvent reorganization energy, λ_s, calculated according to the dielectric continuum model, and in the driving force, ΔG, estimated using the Weller equation (eqs S12–14 in the Supporting Information).

Equation 4 was fitted directly to the femtosecond fluorescence time profiles (Figure 5). Additionally, this equation was integrated to fit the steady-state Stern–Volmer plots (Figures 3 and 4). For the fit, the closest approach distance, r_0, the coupling V and β were adjusted, whereas all the other parameters were either measured directly (n_D, η, excited-state energy) or taken from the literature (ε_s, $E^{ox/red}$).

Table 2 presents a set of parameters, which is able to reproduce very satisfactorily the steady-state Stern–Volmer plots as well as the subnanosecond and femtosecond time-resolved fluorescence profiles (Figures 2 to 5) in all solvents. It should be noted that the k_{diff} values obtained from this DET analysis are somewhat larger (by 50% at most, see Supporting Information) than those calculated from eq 1. This difference stems mainly from the distance dependence of the ET used in the model that results in a quenching radius slightly larger than the contact radius. It is reassuring to find that the obtained contact radius, r_0, is practically equal to the sum of the van der Waals radii of the reactants. In addition, the V_0 and β values are essentially independent of the solvent, ionic or dipolar. This is consistent with the fact that these two quantities are intrinsic parameters of the reactant pair and should mostly depend on the wave functions of reactants and products and their overlap. Moreover, the magnitude of these two quantities is in agreement with previous studies on similar systems and within the range of applicability of the diabatic reaction model used.[49,50] The longitudinal solvent relaxation time, τ_L, of the DMSO/GLY mixture was held constant at the value reported in ref 32, whereas it was allowed to vary freely for the RTILs. The so-obtained τ_L values scale with the viscosity of the RTILs and are comparable to the shortest and medium solvent relaxation times determined experimentally for RTILs but not to the average solvation times.[35,51] This can be due to the fact that in such complex liquids, the relaxation mode associated with the ET reaction may not be unique, as assumed in our model. The variation of the relaxation time with the composition of the DMSO/GLY mixture is still a matter of research, but it has so far been successfully simulated with a single time.[32] This apparent independence of the τ_L value cannot stem from possible differences in the composition of the DMSO/GLY mixture around the reactant pairs as this would also alter the reorientational dynamics of the solutes. However, even in the case of a multiphasic dielectric relaxation, which can be anticipated for DMSO/GLY, one can expect the fastest response to be dominated by DMSO and to have the most prominent impact.[52] In any case, the τ_L values recovered from the RTILs are much longer than those for DMSO/GLY. As a matter of fact, the dielectric relaxation of RTILs has been suggested to be intrinsically different from that of conventional dipolar liquids, as it involves the translational motion of ions rather than the reorientational motion of dipoles.[12,53,54]

Table 2 reveals that the intrinsic ET rate constant, that is, the quenching rate constant in the static regime, k_0, is substantially slower in the RTILs than in the DMSO/GLY mixtures. Such a faster static quenching in the dipolar solvents was already anticipated from the larger curvature of the steady-state Stern–Volmer plots (Figure 3) and the faster early fluorescence dynamics (Figure 5). After this static stage, quenching is dominated by diffusional effects and thus proceeds similarly in RTILs and the DMSO/GLY mixtures of the same viscosity.

The larger intrinsic ET rate constant in DMSO/GLY can have various origins:

(1) The dielectric constants of the RTILs, especially those of EMIDCA and BMIDCA, are smaller than those of the DMSO/GLY mixtures (Chart 1). Because of this, the driving force, $-\Delta G$, decreases in the two less viscous solvents by more than 0.2 eV.

(2) The dielectric solvent relaxation times in the RTILs are substantially larger than those of the DMSO/GLY mixtures. Given the moderate driving force of ET between CNPe and DMA, the stabilization of the ionic product by solvation is crucial and thus the solvent response may become a controlling factor as already observed in many photoinduced charge separation processes in various solvents, including RTILs.[12]

Despite the apparent success of this Marcus-based analysis of the data, one should bear in mind that there are current concerns about its applicability in quantitative terms. The main issue for dispute is based on the use of the continuum dielectric approximation for the description of RTILs.[55] Despite this, previous work by Lynden-Bell suggests its applicability to be granted even for RTILs.[56] In any case, this model gives a very

dx.doi.org/10.1021/ja208265x | J. Am. Chem. Soc. 2012, 134, 3729–3736

consistent rationale of the quenching of CNPe by DMA in all solvents investigated.

It is now possible to explain quantitatively the strong discrepancy found between the quenching rate constants obtained from simple Stern–Volmer analysis, that is, k_q^τ and k_q^s, and the diffusion rate constant, k_{diff}. Figure 6 shows the time dependence of the quenching rate coefficient, $k(t)$, calculated with the best-fit parameters obtained in the three RTILs and in the DMSO/GLY mixtures. In the most viscous RTIL, this constant amounts to $k_0 = 1.5 \times 10^{10}$ M^{-1} s^{-1} at early times and decreases continuously over time to reach a constant value of $k_{diff} = 5 \times 10^7$ M^{-1} s^{-1}. This represents a decrease of the quenching rate by a factor of about 300! However, this variation is relatively slow. As a consequence, only a small part of this change is accessible in a fluorescence quenching experiment, because of the finite lifetime of the excited-state population. Therefore, the slowest decay component of the fluorescence measured in the TCSPC experiment reflects the quenching rate coefficient at a given time depending on the lifetime of the fluorophore but not the stationary value k_{diff} that is attained only after more than a microsecond. This time window shrinks with decreasing fluorescence lifetime. Thus, upon addition of quencher, the effective quenching rate coefficient increases continuously toward k_0. This explains why the quenching rate constant k_q^τ is much larger than k_{diff} and why this difference increases with viscosity.

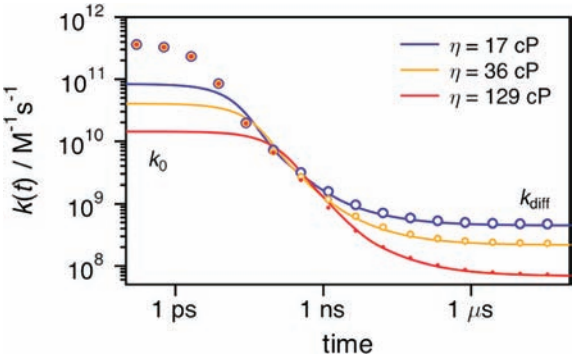

Figure 6. Time dependence of the rate coefficients, $k(t)$, for the solvents studied here, calculated using eq 5 and the parameters listed in Table 2. Full lines correspond to the RTILs, while the circles denote the DMSO/GLY mixtures. Note the identical static quenching rates in all DMSO/GLY mixtures and the diffusion rate constants that depend only on the solvent viscosity, but not on its dipolar or ionic nature.

This relatively slow variation of $k(t)$ has an even more dramatic effect when performing a steady-state Stern–Volmer plot. In this experiment, the measured intensity does not depend on the value of k at a given time but reflects a kind of time-averaged value of k, starting at time zero, where $k = k_0$, to a time t depending on the lifetime of the fluorophore, where $k > k_{diff}$. As the excited-state lifetime decreases with increasing quencher concentration, this averaging is done over a continuously shorter time window and the measured value tends toward k_0. Therefore, the quenching rate constant k_q^s is even larger than k_q^τ.

CONCLUSIONS

The above results show that, at least in the cases studied here, photoinduced bimolecular electron transfer reactions in RTILs are not faster than in conventional solvents but behave as expected for diffusion-controlled processes. In the particular case of electron transfer, the dielectric relaxation of the solvent plays a major role in the control of the reaction rate, and the intrinsic ET rates found here are even faster in conventional polar solvents than in RTILs. However, our experiments do not exclude the existence of specific effects that could, in some special circumstances, result in a faster diffusion.

The difficulty when studying bimolecular quenching processes in RTILs arises from their high viscosity. Because of this, the establishment of the stationary diffusional quenching regime can take several tens of nanoseconds or longer, and as conventional organic fluorophores have an excited-state lifetime of about 10 ns, quenching occurs almost entirely in the static and transient regimes. This results in strongly nonlinear steady-state Stern–Volmer plots that—even at low quencher concentrations—cannot be analyzed with the Stern–Volmer equation. Doing this yields quenching rate constants that are much larger than the stationary rate constant and that depend strongly on the excited-state lifetime of the fluorophore.

As a consequence, there are only two options to obtain reliable rate constants for photoinduced bimolecular reactions in RTILs: (1) use a chromophore with a sufficiently long excited-state lifetime, like a molecule in the triplet state, so that most of the quenching occurs in the stationary regime, with the advantage that the shortening of the long decay component, τ_{long}, in a time-resolved experiment, or the decrease of the steady state intensity, I_{ss}, at low quencher concentration, can be analyzed with the Stern–Volmer equation; or (2) use an ordinary fluorophore with an excited-state lifetime of the order of a few nanoseconds with the consequence that reliable information can only be obtained from the analysis of the fluorescence time profile with a theoretical model accounting for all three quenching regimes, like, for example, DET applied here. The inconvenience of this latter approach lies in the fact that it requires a model for the reaction rate, like the Marcus model used here. However, our study shows that this approach allows for a coherent description of one and the same reaction in solvents of very different viscosity and nature, without the need to invoke any additional extraordinary effects for only a few solvents.

ASSOCIATED CONTENT

Supporting Information

Femtosecond time-resolved anisotropy decays. Details on data treatment and the theoretical model. Transient absorption spectra in EMIDCA. This material is available free of charge via the Internet at http://pubs.acs.org.

AUTHOR INFORMATION

Corresponding Author

E-mail: eric.vauthey@unige.ch

Notes

The authors declare no competing financial interest.

ACKNOWLEDGMENTS

This work was supported by the Fonds National Suisse de la Recherche Scientifique through the NCCR MUST and the University of Geneva.

REFERENCES

(1) Plechkova, N. V.; Seddon, K. R. *Chem. Soc. Rev.* **2008**, *37*, 123.

(2) Welton, T. *Chem. Rev.* **1999**, *99*, 2071.
(3) Wishart, J. F. *Energy Environ. Sci.* **2009**, *2*, 956.
(4) Hallett, J. P.; Welton, T. *Chem. Rev.* **2011**, *111*, 3508.
(5) Bai, Y.; Cao, Y.; Zhang, J.; Wang, M.; Li, R.; Wang, P.; Zakeeruddin, S. M.; Grätzel, M. *Nat. Mater.* **2008**, *7*, 626.
(6) Bai, Y.; Zhang, J.; Wang, Y.; Zhang, M.; Wang, P. *Langmuir* **2011**, *27*, 4749.
(7) Hardin, B. E.; Sellinger, A.; Moehl, T.; Humphry-Baker, R.; Moser, J.-E.; Wang, P.; Zakeeruddin, S. M.; Grätzel, M.; McGehee, M. D. *J. Am. Chem. Soc.* **2011**, *133*, 10662.
(8) Castner, E. W.; Wishart, J. F. *J. Chem. Phys.* **2010**, *132*, 120901.
(9) Castner, E. W.; Margulis, C. J.; Maroncelli, M.; Wishart, J. F. *Annu. Rev. Phys. Chem.* **2011**, *62*, 85.
(10) Lockard, J. V.; Wasielewski, M. R. *J. Phys. Chem. B* **2007**, *111*, 11638.
(11) Banerji, N.; Angulo, G.; Barabanov, I. I.; Vauthey, E. *J. Phys. Chem. A* **2008**, *112*, 9665.
(12) Li, X.; Liang, M.; Chakraborty, A.; Kondo, M.; Maroncelli, M. *J. Phys. Chem. B* **2011**, *115*, 6592.
(13) Skrzypczak, A.; Neta, P. *J. Phys. Chem. A* **2003**, *107*, 7800.
(14) Paul, A.; Samanta, A. *J. Phys. Chem. B* **2007**, *111*, 1957.
(15) Vieira, R. C.; Falvey, D. E. *J. Phys. Chem. B* **2007**, *111*, 5023.
(16) Vieira, R. C.; Falvey, D. E. *J. Am. Chem. Soc.* **2008**, *130*, 1552.
(17) Sarkar, S.; Pramanik, R.; Seth, D.; Setua, P.; Sarkar, N. *Chem. Phys. Lett.* **2009**, *477*, 102.
(18) Sarkar, S.; Pramanik, R.; Ghatak, C.; Rao, V. G.; Sarkar, N. *J. Chem. Phys.* **2011**, *134*, 074507/1.
(19) Rice, S. A. *Comprehensive Chemical Kinetics, Vol 25. Diffusion Limited Reactions*; Elsevier: New York, 1985.
(20) Eads, D. D.; Dismer, B. G.; Fleming, G. R. *J. Chem. Phys.* **1990**, *93*, 1136.
(21) Murata, S.; Matsuzaki, S. Y.; Tachiya, M. *J. Phys. Chem.* **1995**, *99*, 5354.
(22) Murata, S.; Tachiya, M. *J. Phys. Chem.* **1996**, *100*, 4064.
(23) Zhou, H. X.; Szabo, A. *Biophys. J.* **1996**, *71*, 2550.
(24) Weidemaier, K.; Tavernier, H. L.; Swallen, S. F.; Fayer, M. D. *J. Phys. Chem. A* **1997**, *101*, 1887.
(25) Burel, L.; Mostafavi, M.; Murata, S.; Tachiya, M. *J. Phys. Chem. A* **1999**, *103*, 5882.
(26) Burshtein, A. I. *Adv. Chem. Phys.* **2004**, *129*, 105.
(27) Neufeld, A. A.; Burshtein, A. I.; Angulo, G.; Grampp, G. *J. Chem. Phys.* **2002**, *116*, 2472−2479.
(28) Angulo, G. Ph.D. thesis, Technical University Graz, 2003.
(29) Angulo, G.; Grampp, G.; Neufeld, A. A.; Burshtein, A. I. *J. Phys. Chem.* **2003**, *107*, 6913.
(30) Gladkikh, V. S.; Burshtein, A. I.; Angulo, G.; Grampp, G. *Phys. Chem. Chem. Phys.* **2003**, *5*, 2581.
(31) Rosspeintner, A.; Kattnig, D. R.; Angulo, G.; Landgraf, S.; Grampp, G.; Cuetos, A. *Chem.—Eur. J.* **2007**, *13*, 6474.
(32) Angulo, G.; Kattnig, D. R.; Rosspeintner, A.; Grampp, G.; Vauthey, E. *Chem.—Eur. J.* **2010**, *16*, 2291.
(33) Morandeira, A.; Fürstenberg, A.; Gumy, J.-C.; Vauthey, E. *J. Phys. Chem. A* **2003**, *107*, 5375.
(34) Riddick, J. A.; Bunger, W. B. *Organic Solvents*; J. Wiley: New York, 1970.
(35) Hunger, J.; Stoppa, A.; Schrödle, S.; Hefter, G.; Buchner, R. *ChemPhysChem* **2009**, *10*, 723.
(36) Huang, M.-M.; Jiang, Y.; Sasisanker, P.; Driver, G. W.; Weingärtner, H. *J. Chem. Eng. Data* **2011**, *56*, 1494.
(37) Buu-Hoï, N. P.; Long, C. T. *Recl. Trav. Chim. Pays-Bas* **1956**, *75*, 1221.
(38) Muller, P.-A.; Högemann, C.; Allonas, X.; Jacques, P.; Vauthey, E. *Chem. Phys. Lett.* **2000**, *326*, 321.
(39) Morandeira, A.; Engeli, L.; Vauthey, E. *J. Phys. Chem. A* **2002**, *106*, 4833.
(40) Gladkikh, V. S.; Burshtein, A. I.; Tavernier, H. L.; Fayer, M. D. *J. Phys. Chem. A* **2002**, *106*, 6982.
(41) Collins, F. C.; Kimball, G. E. *J. Colloid Sci.* **1949**, *4*, 425.
(42) Swallen, S. F.; Weidemaier, K.; Fayer, M. D. *J. Chem. Phys.* **1996**, *104*, 2976.
(43) Marcus, R. A.; Sutin, N. *Biochim. Biophys. Acta* **1985**, *811*, 265.
(44) Yakobson, B. I.; Burshtein, A. I. *Chem. Phys.* **1980**, *49*, 385.
(45) Zusman, L. D. *Chem. Phys.* **1980**, *49*, 295.
(46) Rips, I.; Jortner, J. *J. Chem. Phys.* **1987**, *87*, 2090.
(47) Heitele, H. *Angew. Chem., Int. Ed. Engl.* **1993**, *32*, 359.
(48) Marcus, Y. *The Properties of Solvents*; Wiley: New York, 1998.
(49) Barzykin, A. V.; Frantsuzov, P. A.; Seki, K.; Tachiya, M. *Adv. Chem. Phys.* **2002**, *123*, 511.
(50) Gladkikh, V. S.; Burshtein, A. I.; Rips, I. *J. Phys. Chem. A* **2005**, *109*, 4983.
(51) Jin, H.; Baker, G. A.; Arzhantsev, S.; Dong, J.; Maroncelli, M. *J. Phys. Chem. B* **2007**, *111*, 7291.
(52) Hynes, J. T. *J. Phys. Chem.* **1986**, *90*, 3701.
(53) Shim, Y.; Choi, M. Y.; Kim, H. J. *J. Chem. Phys.* **2005**, *122*, 044511.
(54) Kobrak, M. N. *J. Chem. Phys.* **2006**, *125*, 064502/1.
(55) Kobrak, M. N.; Li, H. *Phys. Chem. Chem. Phys.* **2010**, *12*, 1922.
(56) Lynden-Bell, R. M. *J. Phys. Chem. B* **2007**, *111*, 10800.